Chemistry–A European Journal

Research Article
doi.org/10.1002/chem.202500462

Chemistry Europe
European Chemical Societies Publishing

www.chemeurj.org

The Synthesis of Hydroquinolines from Nitroaldehydes and Ketones by Hydrogenation Sequences and Condensations

Christof Bauer[+],[a] Fatemeh Zareh[+],[a] Lisa Nüßlein,[a] Johanna Frank,[a] Maxime Boniface,[b] Thomas Lunkenbein,[b] and Rhett Kempe*[a]

Catalytic reaction discovery or methodology development is preferably performed with homogeneous catalysts, but heterogeneous catalysts allow the design of complex multistep syntheses based on their reusability. We introduce here the catalytic synthesis of hydroquinolines starting from nitroaldehydes, ketones and hydrogen. The reaction is complex and proceeds via multiple selective hydrogenation and condensation steps. The nitroaldehyde is selectively hydrogenated forming an aminoaldehyde, followed by a base-catalyzed *Friedländer* synthesis and selective quinoline hydrogenation. The starting materials are inexpensive, simple regarding their structure and diversely available, and the hydroquinoline motif is part of numerous biologically active compounds. A nanostructured earth-abundant metal catalyst mediates our reaction most efficiently.

Introduction

The discovery of catalytic reactions or methodology development is preferentially carried out with homogeneous catalysts.[1] Homogeneous or molecular catalysts are easily modified to provide the activity and selectivity required to mediate novel chemical reactions. In addition, detailed (structural) characterization of active catalysts is easier in comparison to heterogeneous or enzyme catalysts.[2] Heterogeneous catalysts, if reusable, can not only be used several times for the same reaction but also in different reactions sequentially.[3] This quality might open perspectives to rationally design and mediate complex chemical reactions. We have introduced a complex condensation reaction where reusable noble metal catalysts were added and removed to mediate a multistep hydrogenation and dehydrogenation sequence[4] and report here the direct synthesis of hydroquinolines starting from nitroaldehydes and ketones and (no break here)hydrogen (Figure 1). The starting materials of our reaction are inexpensive, simple regarding their structure and diversely available, and the hydroquinoline motif is important, figures prominently among pharmaceuticals (Figure 1a) and its synthesis is intensively investigated.[5] Our reaction proceeds via multiple selective hydrogenation and condensation steps. The nitroaldehyde is selectively hydrogenated to an aminoaldehyde[6] (Figure 1b) followed by a base-catalyzed *Friedländer* synthesis[7] (Figure 1c) forming a quinoline and a final selective quinoline hydrogenation step[8] (Figure 1d). A novel reusable nickel catalyst mediates all hydrogenation steps selectively. The reaction has a broad scope, an attractive functional group tolerance and upscaling has been demonstrated.

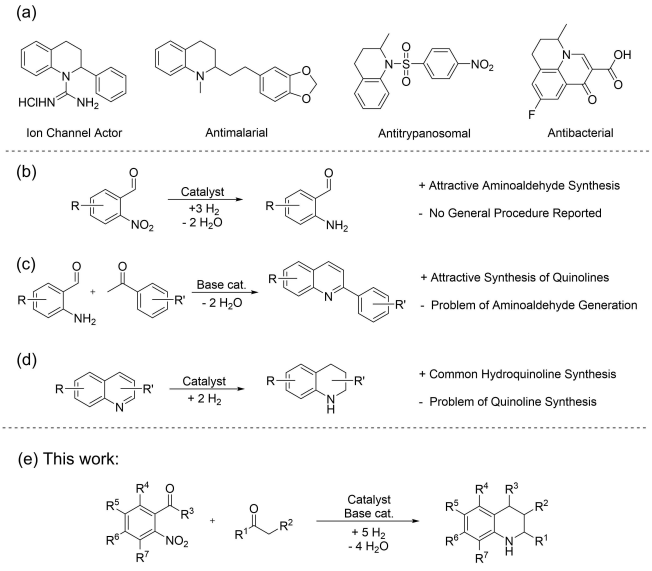

Figure 1. State of the art and reaction reported here. (a) Selection of bioactive molecules with a 1,2,3,4-tetrahydroquinoline motif. (b) Selective hydrogenation of 2-nitrobenzaldehyde to 2-aminobenzaldehyde. (c) *Friedländer* synthesis. (d) Selective hydrogenation of 2-phenylquinoline to 2-phenyl-1,2,3,4-tetrahydroquinoline. (e) The direct synthesis of tetrahydroquinolines.

[a] *C. Bauer,[+] F. Zareh,[+] L. Nüßlein, J. Frank, Prof. Dr. R. Kempe*
Inorganic Chemistry II – Catalyst Design
Sustainable Chemistry Centre
University of Bayreuth
95440 Bayreuth (Germany)
E-mail: kempe@uni-bayreuth.de
Homepage: www.sustainable-chemistry-centre.uni-bayreuth.de

[b] *Dr. M. Boniface, Dr. T. Lunkenbein*
Fritz Haber Institute of the Max Planck Society
Department of Inorganic Chemistry
14195 Berlin (Germany)

[+] *These authors contribute equally.*

Supporting information for this article is available on the WWW under https://doi.org/10.1002/chem.202500462

Results and Discussion

Catalyst Synthesis and Characterization

The synthesis of our catalyst is shown in Figure 2a. The catalyst support material N-SiC (a porous N-doped and Si-coated carbon) was synthesized according to a procedure published previously (Supporting Information 2.1).[9] Cross-linking of the commercially available polycarbosilane precursor SMP-10 and acrylonitrile using azobis(isobutyronitrile), pyrolysis and the removal of the Si-rich phase by base treatment are the N-SiC synthesis steps. The N-SiC support material was wet impregnated with a solution of $Ni(NO_3)_2 \cdot 6\ H_2O$ in water, followed by pyrolysis (700 °C) under nitrogen flow and reduction (550 °C) under forming gas (N_2:H_2, 90:10) to form the Ni/N-SiC catalyst (Figure 2b and Supporting Information 2.2). Inductively coupled plasma optical emission spectrometry analysis of Ni/N-SiC showed no significant deviation from the theoretical nickel content of 4.0 wt% (Supporting Information 3.1). Elemental analysis revealed that Ni/N-SiC consists of 83.3% C, 5.7% N and 7.0% Si in addition to nickel (Supporting Information 3.2). Scanning electron microscopy in combination with energy dispersive X-ray spectroscopy (SEM-EDX) confirmed the homogeneous distribution of nickel over N-SiC (Supporting Information 3.3) and verified a smooth wet impregnation process. Scanning transmission electron microscopy (STEM) in combination with high-angle annular dark-field (HAADF) imaging analysis revealed a homogeneous distribution of nanoparticles over the support material (Figure 2b–c) and an average particle size of 8.5 nm (Figure 2d). The presence of nickel nanoparticles was confirmed using HAADF-STEM in combination with EDX element maps (Figure 2e–h). High resolution transmission electron microscopy in combination with electron energy loss spectroscopy (EELS) with a line scan over one nickel nanoparticle was performed next (Supporting Information 3.5). The resulting EELS spectrum and the calculated $Ni(L_3)$: $Ni(L_2)$ intensity ration of 1.38 fit to the literature value consistent with metallic Ni.[10] In addition, no oxygen was detected in the STEM-EELS measurements. We propose that Ni/N-SiC consist of metallic nickel nanoparticles supported by N-SiC. Fast Fourier transformation of a single nickel nanoparticle (Supporting Information 3.6) indicates cubic nickel. (no break here)X-ray photoelectron spectroscopy (XPS) was performed to study the surface of the cubic nickel nanoparticles (Supporting Information 3.7). The spectra were measured before and after Pt sputtering. The pre-sputtering spectrum shows the presence of metallic nickel (49%) and nickel oxide (51%), while after sputtering, the metallic nickel content increases to 89% and the nickel oxide content decreases to 11%. We assume that the nickel nanoparticles are surrounded by a very thin layer of

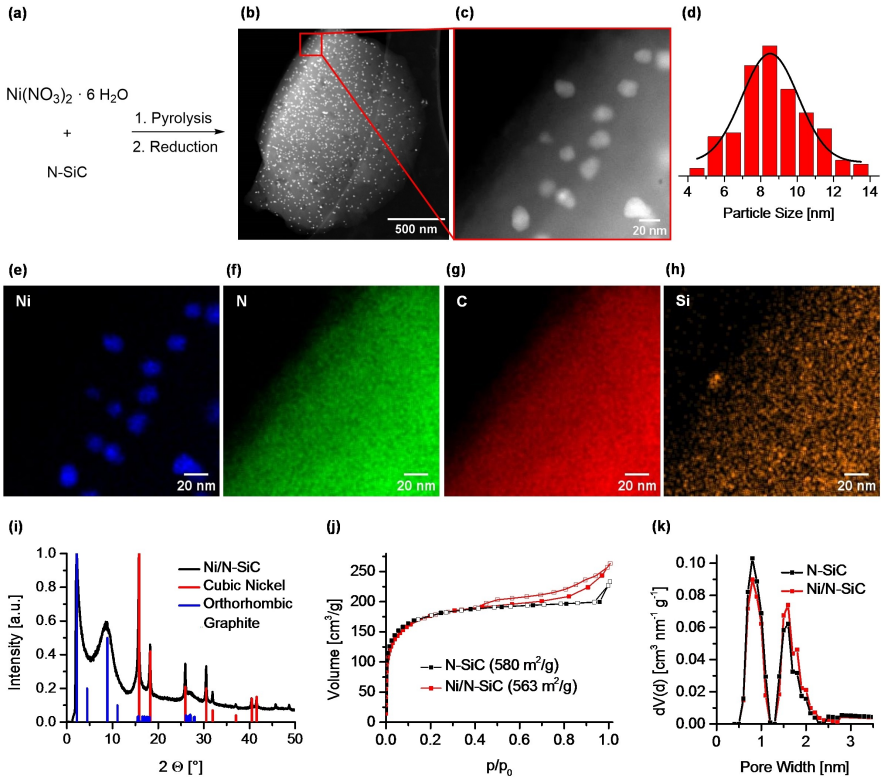

Figure 2. Synthesis and characterization of the Ni/N-SiC catalyst. (a) Synthesis of the Ni/N-SiC catalyst: Wet impregnation of N-SiC with aqueous solution of $Ni(NO_3)_2 \cdot 6\ H_2O$, pyrolysis and reduction. (b) HAADF-STEM analysis suggests the presence of homogeneously distributed nanoparticles. (c) Close-up of the HAADF-STEM. (d) Nanoparticle distribution with an average particle size of 8.5 nm (150 particles counted). (e–h) HAADF-STEM images of Ni/N-SiC with representative EDX element maps of nickel (e), nitrogen (f), carbon (g) and silicon (h). (i) PXRD of the Ni/N-SiC catalyst (black). The reflexes match those of cubic nickel (red, reference code: 00-004-0850). (j) Surface characterization and (k) pore size distribution of the catalyst via Ar physisorption measurements (calculation model: Ar at −186.15 °C on carbon: cylindric pores, non-local density functional theory equilibrium model). The specific surface area showed a slight decrease from 580 m^2/g of the support material to 563 m^2/g of the catalyst.

nickel oxide. Powder X-ray diffraction (PXRD) of Ni/N-SiC (Figure 2i) confirms cubic nickel (red) and orthorhombic graphite (blue). The specific surface area was determined by argon physisorption measurements (Figure 2j), which showed a slight decrease of the surface area from 580 m^2/g of the N-SiC support to 563 m^2/g of the catalyst. The pore size distribution of Ni/N-SiC (Figure 2k) shows a predominance of micropores.

Optimization of Reaction Conditions

The reaction of 2-nitrobenzaldehyde with acetophenone to form 2-phenyl-1,2,3,4-tetrahydroquinoline was chosen to determine suitable reaction conditions. The reaction is complex and consists of three steps: the hydrogenation of nitrobenzaldehydes to aminobenzaldehydes (A), the *Friedländer* synthesis (B) and the hydrogenation of quinolines to 1,2,3,4-tetrahydroquinolines (C). A screening of different solvents revealed that 3 mL ethanol is the best solvent for all three steps (Table S2–S3). Several types of bases were investigated, with LiOH being the best base used in a catalytic amount (Table S4–S5). The amount of base seems to have an optimum. More base accelerates the condensation steps but slows down the final hydrogenation step. Investigation of the H_2 pressure, if needed, and time and temperature revealed that the best conditions for step A are 40 °C at 3.0 MPa hydrogen pressure for 20 h (Table S6–S7). The best yield for step B was obtained at 60 °C for 20 h (Table S8), and 120 °C with 5.0 MPa hydrogen pressure for 48 h (Table S9–S10) gave the best results for step C. Next, the pyrolysis temperature for the catalyst synthesis was varied and different commercially available support materials and nickel precursors were tested for the overall reaction (Table 1). Lowering the pyrolysis temperature below 700 °C reduced the yield obtained, as did pyrolysis temperatures above 700 °C. Different catalyst

Table 1. Nickel catalyst screening.[a]

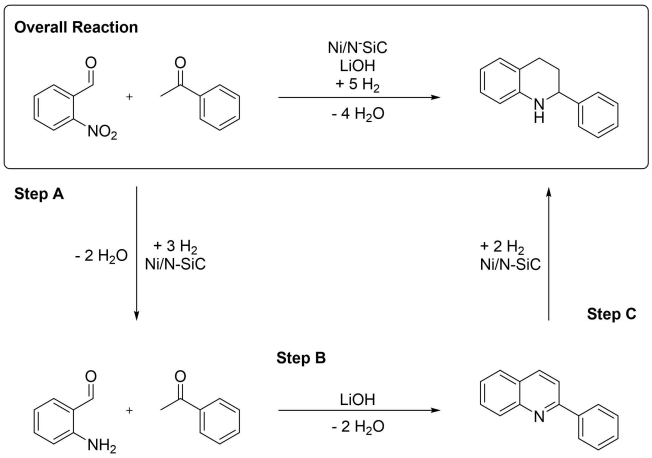

Entry	Metal Source	Support Material	Pyrolysis Temperature [°C]	Yield [%]
1	$Ni(NO_3)_2 \cdot 6\ H_2O$	N-SiC	500	45
2	$Ni(NO_3)_2 \cdot 6\ H_2O$	N-SiC	600	48
3	**$Ni(NO_3)_2 \cdot 6\ H_2O$**	**N-SiC**	**700**	**91**
4	$Ni(NO_3)_2 \cdot 6\ H_2O$	N-SiC	800	28
5	$Ni(NO_3)_2 \cdot 6\ H_2O$	N-SiC	900	8
6	$Ni(NO_3)_2 \cdot 6\ H_2O$	Activated Carbon	700	6
7	$Ni(NO_3)_2 \cdot 6\ H_2O$	γ-Al_2O_3	700	0
8	$Ni(NO_3)_2 \cdot 6\ H_2O$	TiO_2	700	0
9	$Ni(NO_3)_2 \cdot 6\ H_2O$	SiO_2	700	0
10	$Ni(NO_3)_2 \cdot 6\ H_2O$	CeO_2	700	0
11	$Ni(OAc)_2 \cdot 4\ H_2O$	N-SiC	700	4
12	$Ni(acac)_2 \cdot 2\ H_2O$	N-SiC	700	51
13	Ni(II)stearate	N-SiC	700	12
14	$NiCl_2 \cdot 6\ H_2O$	N-SiC	700	4
15	–	N-SiC	700	0

[a] Reaction conditions: Step A: 4 mol% Ni/N-SiC (0.02 mmol Ni, 1.17 mg Ni), 0.5 mmol 2-nitrobenzaldehyde, 0.5 mmol acetophenone, 3 mL ethanol, 3.0 MPa H_2, 40 °C for 20 h. Step B: Addition of 0.3 mmol LiOH then 60 °C for 20 h. Step C: 5.0 MPa H_2, 120 °C for 48 h. Yields were determined by GC using *n*-dodecane as an internal standard.

support materials, such as activated carbon, γ-Al_2O_3, TiO_2, SiO_2 and CeO_2, were investigated. They all showed no activity, except for activated carbon with a very low yield of 6%. The use of nickel nitrate as a metal precursor is important for the superior activity and selectivity of our catalyst. Only a little activity was observed for the metal precursors nickel acetate, nickel stearate and nickel chloride. An important issue is the smooth impregnation including the solubility of the nickel salt used. It is solely the nickel acetylacetonate precursor that shows a higher yield, with 51% of the product of interest. Variation of the catalyst metal loading revealed that a catalyst with 4.0 wt% nickel is optimal (Table S11) and 4.0 mol% Ni was identified as the catalyst loading for the three reaction steps (Table S12). Time conversion studies (Supporting Information 4.2) showed that step A is complete after 15 h under the optimal reaction conditions applied. The complete conversion of 2-aminobenzaldehyde with acetophenone to 2-phenylquinoline is achieved after 14 h in step B. The selective hydrogenation of 2-phenylquinoline to 2-phenyl-1,2,3,4-tetrahydroquinoline, step C, is the most demanding step of the overall reaction. A maximum yield of 91% was obtained after 42 h. In summary, the overall reaction can be carried out applying the following reaction conditions: Step A: 4.0 mol% Ni (4.0 wt% Ni), 0.5 mmol 2-nitrobenzaldehyde, 0.5 mmol acetophenone, 3 mL ethanol, 3.0 MPa H_2, 40 °C and 20 h reaction time. Step B: Addition of 0.6 eq LiOH and 20 h reaction time. Step C: 5.0 MPa H_2, 120 °C and 48 h reaction time. Starting the reaction with step B is challenging since there is no general amino aldehyde synthesis.

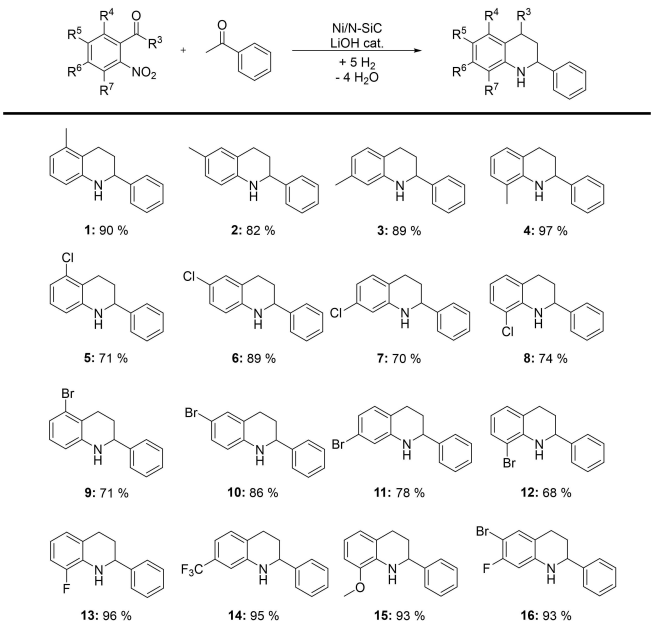

Scheme 1. Direct synthesis of hydroquinolines with acetophenone and variation of the nitroaldehyde educts. Reaction conditions: Step A: 29.3 mg Ni/N-SiC catalyst (4 mol% Ni, 0.02 mmol Ni, 1.17 mg Ni), 0.5 mmol 2-nitrobenzaldehyde, 0.5 mmol acetophenone, 3 mL ethanol, 3.0 MPa H_2, 40 °C for 20 h. Step B: Addition of 0.3 mmol LiOH. Then 60 °C for 20 h. Step C: 5.0 MPa H_2, 120 °C for 48 h. Isolated yields are given.

Substrate Scope

With the optimized reaction conditions in hand, we became interested in the applicability of our complex reaction. Aldehyde variations employing acetophenone are shown in Scheme 1. Firstly, we applied our protocol to synthesize products carrying electron-donating methyl substituents. The products desired were obtained in mostly very good yields and any position on the aryl ring of the 2-nitrobenzaldehyde derivatives could be addressed (Scheme 1, products **1**–**4**). In addition, we can tolerate electron-withdrawing substituents and, again, any position on the aryl ring of the 2-nitrobenzaldehyde could be tolerated (Scheme 1, products **5**–**12**), albeit lower product yields were obtained. Furthermore, 8-fluoro-2-phenyl-1,2,3,4-tetrahydroquinoline was synthesized in a 96% isolated yield (Scheme 1, product **13**) and a CF_3 group was tolerated and an isolated yield of 95% was obtained (Scheme 1, product **14**). Moreover, we successfully synthesized 8-methoxy-2-phenyl-1,2,3,4-tetrahydroquinoline in a 93% isolated yield (Scheme 1, product **15**), and a product bearing two different functional groups was also introduced (Scheme 1, product **16**).

We next investigated the ketone variation (Scheme 2). We used the same conditions and isolated 21 different products. Electron-donating methyl groups in the *para*-, *meta*- and *ortho*-positions of the 2-phenyl substituent of the 1,2,3,4-tetrahydroquinoline were well tolerated (Scheme 2, products **17**–**19**).

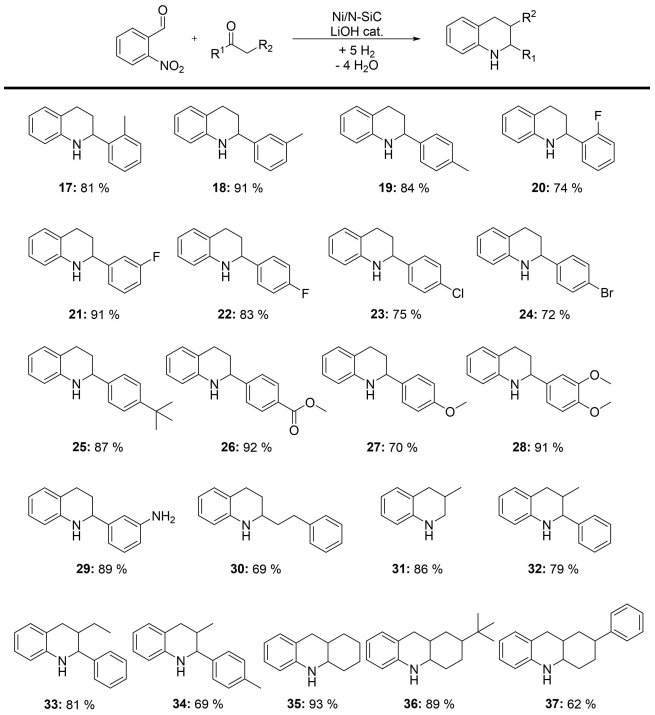

Scheme 2. Direct synthesis of hydroquinolines with 2-nitrobenzaldehyde and a variation of the ketone educt. Reaction conditions: Step A: 29.3 mg Ni/N-SiC catalyst (4 mol% Ni, 0.02 mmol Ni, 1.17 mg Ni), 0.5 mmol 2-nitrobenzaldehyde, 0.5 mmol ketone, 3 mL ethanol, 3.0 MPa H_2, 40 °C for 20 h. Step B: Addition of 0.3 mmol LiOH. Then 60 °C for 20 h. Step C: 5.0 MPa H_2, 120 °C for 48 h. Isolated yields are given.

Similarly, it is possible to incorporate electron-withdrawing groups and products with fluoro substituents in the *para*-, *meta*- and *ortho*-positions of the 2-phenyl substituent which were synthesized (Scheme 2, products **20–22**). The conversion of 2-fluoroacetophenone with 2-nitrobenzaldehyde was the most challenging and resulted in an isolated product yield of 74%. We assume that the combination of electron-withdrawing and steric hindrance is challenging. Chloro- (Scheme 2, product **23**) and bromo-substituted (Scheme 2, product **24**) products could be synthesized. Note that the difficulty of introducing halogen-substituted educts into the procedure due to the harsh conditions in step C did not occur in a large quantity. The *tert*-butyl group could be introduced, giving 2-(4-(*tert*-butyl)phenyl)-1,2,3,4-tetrahydroquinoline in an 87% yield (Scheme 2, product **25**) and a 1,2,3,4-tetrahydroquinoline bearing an acetate group on the phenyl ring was also obtained in a very good yield (Scheme 2, product **26**). Methoxy groups are tolerated and a dimethoxy derivative gives a higher yield (91%, product **28**) than a monomethoxy derivative (70%, product **27**). The synthesis protocol is also successful when an amine group is present (Scheme 2, product **29**). We next investigated the synthesis of alkyl-substituted hydroquinolines: 2-phenethyl-1,2,3,4-tetrahydroquinoline (Scheme 2, product **30**) and 3-methyl-1,2,3,4-tetrahydroquinoline (Scheme 2, product **31**) were synthesized. The latter example shows that we can use two aldehydes in our catalytic synthesis. Furthermore, various 2,3-disubstituted products, including three-cyclic products, were synthesized (Scheme 2, products **32** to **37**). Aldehyde and ketone can be varied simultaneously and we obtained 6-fluoro-2-(*para*-tolyl)-1,2,3,4-tetrahydroquinoline in a 72% yield (Scheme 3, product **38**). Moreover, 1,2,3,4-tetrahydroquinoline with up to four different substituents was synthesized (Scheme 3, product **39** and **40**).

Our hydroquinoline synthesis is also interesting in terms of applications (synthesis of biologically active ingredients [of drug molecules], Scheme 3). Our benchmark substrate, product **41**, can be easily converted into an ion channel inhibitor in one step.[11] 2-(2-(benzo[*d*][1,3]dioxol-5-yl)ethyl)-1,2,3,4-tetrahydroquinoline (Product **42**), which we synthesized in an 83% isolated yield, can be easily converted to galipinine.[12] Alkaloids from *Galipea officinalis* have long been known for their medicinal effects and galipinine acts as an antiplasmodial and cytotoxic agent against malaria. Product **43**, synthesized from 2-nitrobenzaldehyde and acetone in an 80% yield, can be converted into the active ingredient of an antiparasitic drug.[13] The synthesized 6-fluoro-2-methyl-1,2,3,4-tetrahydroquinoline (Product **44**, 85% yield) can be converted to flumequine, which has antimicrobial activity, can be used as an antibacterial agent and was first synthesized in 1972.[14]

An upscaling of the benchmark reaction was performed using 10 mmol of 2-nitrobenzaldehyde and 10 mmol of acetophenone. An isolated yield of 86% of 2-phenyl-1,2,3,4-tetrahydroquinoline was observed (Supporting Information 4.3). Examinations of the catalyst after the direct synthesis of hydroquinolines by TEM showed no agglomeration or growth of the nickel nanoparticles of the catalyst used. Moreover, the particle size distribution remains constant, with an average particle diameter of 8.5 nm (Supporting Information 4.5.1). A hot filtration test was subsequently conducted. The separated solution showed no activity and the formation of other products was not observed (Supporting Information 4.5.2). Investigation of leaching via ICP-OES suggested negligible leaching and reusability test indicated very good reusability.

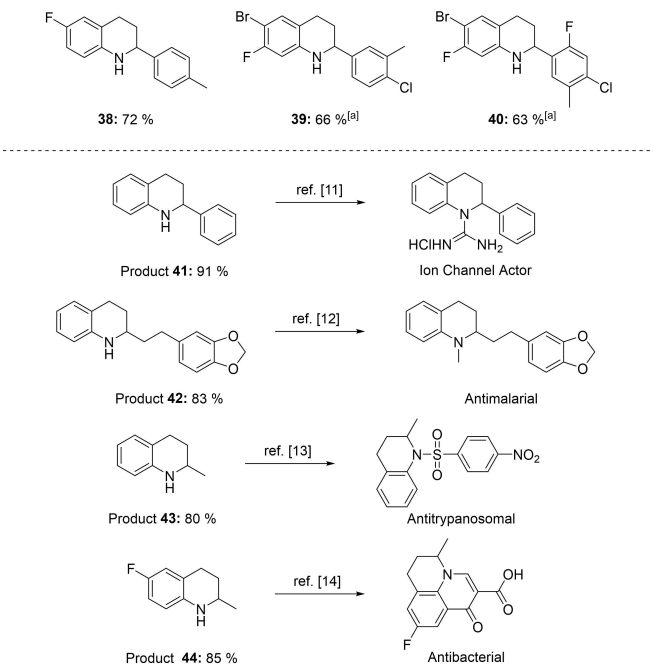

Scheme 3. Highly functionalized 1,2,3,4-tetrahydroquinolines varying both aldehyde and ketone sides and applications of synthesized substrates as precursors for drug molecules. Reaction conditions: Step A: 29.3 mg Ni/N-SiC catalyst (4 mol% Ni, 0.02 mmol Ni, 1.17 mg Ni), 0.5 mmol aldehyde, 0.5 mmol ketone, 3 mL ethanol, 3.0 MPa H_2, 40 °C for 20 h. Step B: Addition of 0.3 mmol LiOH. Then 60 °C, for 20 h. Step C: 5.0 MPa H_2, 120 °C for 48 h. [a] Step B: 1.5 mmol LiOH. Isolated yields are given.

Conclusions

In summary, we report a complex catalytic reaction mediated by a reusable earth-abundant metal catalyst and a simple base (catalyst). The reaction was designed to permit the conversion of inexpensive, structurally simple and diversely available starting materials (nitroaldehydes, ketones and hydrogen) into an important class of N-heterocyclic compounds, namely, hydroquinolines.

Acknowledgements

We thank the SFB 1585 Project A02, 492723217 for financial support. M.B. and T.L. acknowledge the Federal Ministry of Education and Research in the framework of the Catlab project (03EW0015A). In addition, the authors thank F. Baier for XPS measurements, Dr. U. Lacher for HRMS analysis and Dr. C. Denner for SEM-EDX measurements and the Bavarian Polymer Institute (University of Bayreuth, KeyLab Electron and Optical

Microscopy) for assistance with TEM and SEM-EDX measurements. Open Access funding enabled and organized by Projekt DEAL.

Conflict of Interests

The authors declare no conflict of interest.

Data Availability Statement

The data that support the findings of this study are available in the supplementary material of this article.

Keywords: condensation/synthesis · heterogeneous catalysis · hydrogenation · hydroquinolines · nickel

[1] a) T. Zhang, Z. Zhang, G. Kang, T. Sheng, J. Yan, Y. Yang, Y. Ouyang, J. Yu, *Science* **2024**, *384*, 793–798; b) J.-J. Chen, J.-H. Fang, X.-Y. Du, J.-Y. Zhang, J.-Q. Bian, F.-L. Wang, C. Luan, W.-L. Liu, J.-R. Liu, X.-Y. Dong, et al., *Nature* **2023**, *618*, 294–300; c) C. Chen, G. C. Fu, *Nature* **2023**, *618*, 301–307; d) B. Ramadoss, Y. Jin, S. Asako, L. Ilies, *Science* **2022**, *375*, 658–663; e) F. Le Vaillant, A. Mateos Calbet, S. González-Pelayo, E. J. Reijerse, S. Ni, J. Busch, J. Cornella, *Nature* **2022**, *604*, 677–683; f) T. Dietel, F. Lukas, W. P. Kretschmer, R. Kempe, *Science* **2022**, *375*, 1021–1024.

[2] B. Cornils, W. A. Herrmann, J.-H. Xu, H.-W. Zanthoff, *Catalysis from A to Z*, Wiley-VCH, **2020**.

[3] a) R. V. Jagadeesh, K. Murugesan, A. S. Alshammari, H. Neumann, M.-M. Pohl, J. Radnik, M. Beller, *Science* **2017**, *358*, 326–332; b) F. A. Westerhaus, R. V. Jagadeesh, G. Wienhöfer, M.-M. Pohl, J. Radnik, A.-E. Surkus, J. Rabeah, K. Junge, H. Junge, M. Nielsen, et al., *Nat. Chem.* **2013**, *5*, 537–543; c) R. V. Jagadeesh, A.-E. Surkus, H. Junge, M.-M. Pohl, J. Radnik, J. Rabeah, H. Huan, V. Schünemann, A. Brückner, M. Beller, *Science* **2013**, *342*, 1073–1076; d) G. Hahn, P. Kunnas, N. de Jonge, R. Kempe, *Nat. Catal.* **2019**, *2*, 71–77; e) J.-L. Sun, H. Jiang, P. H. Dixneuf, M. Zhang, *J. Am. Chem. Soc.* **2024**, *146*, 11289–11298; f) H. Hua, C. Ci, P. H. Dixneuf, M. Zhang, *J. Am. Chem. Soc.* **2025**, *147*, 6572–6582.

[4] D. Forberg, T. Schwob, R. Kempe, *Nat. Commun.* **2018**, 1751.

[5] a) J. J. Melder, M. L. Heldner, R. Kugler, L. A. Ziegenhagen, F. Rominger, M. Rudolph, A. S. K. Hashmi, *J. Am. Chem. Soc.* **2024**, *146*, 14521–14527; b) G. J. Sherborne, P. Kemmitt, C. Prentice, E. Zysman-Colman, A. D. Smith, C. Fallan, *Angew. Chem. Int. Ed.* **2023**, *62*, e202207829; c) P. Rojo, M. Molinari, A. Cabré, C. García-Mateos, A. Riera, X. Verdaguer, *Angew. Chem. Int. Ed.* **2022**, *61*, e202204300; d) S. Guo, Y. Wu, C. Wang, Y. Gao, M. Li, B. Zhang, C. Liu, *Nat. Commun.* **2022**, *13*, 5297; e) X. Xu, X. Zheng, X. Xu, *ACS Catal.* **2021**, *11*, 14995–15003; f) Z. Han, G. Liu, X. Yang, X.-Q. Dong, X. Zhang, *ACS Catal.* **2021**, *11*, 7281–7291; g) X. Feng, Y. Song, W. Lin, *J. Am. Chem. Soc.* **2021**, *143*, 8184–8192; h) L. Qi, J. Chen, B. Zhang, R. Nie, Z. Qi, T. Kobayashi, Z. Bao, Q. Yang, Q. Ren, Q. Sun, et al., *ACS Catal.* **2020**, *10*, 5707–5714; i) V. Papa, Y. Cao, A. Spannenberg, K. Junge, M. Beller, *Nat. Catal.* **2020**, *3*, 135–142; j) J. Zhang, Z. An, Y. Zhu, X. Shu, H. Song, Y. Jiang, W. Wang, X. Xiang, L. Xu, J. He, *ACS Catal.* **2019**, *9*, 11438–11446.

[6] D. Formenti, F. Ferretti, F. K. Scharnagl, M. Beller, *Chem. Rev.* **2019**, *119*, 2611–2680.

[7] a) P. Friedlaender, *Ber. Dtsch. Chem. Ges.* **1882**, *15*, 2572–2575; b) P. Friedländer, C. F. Gohring, *Ber. Dtsch. Chem. Ges.* **1883**, *16*, 1833–1839.

[8] a) H. Adkins, H. I. Cramer, *J. Am. Chem. Soc.* **1930**, *52*, 4349–4358; b) H. Adkins, H. R. Billica, *J. Am. Chem. Soc.* **1948**, *70*, 695–698; c) J. E. Shaw, P. R. Stapp, *J. Heterocycl. Chem.* **1987**, *24*, 1477–1483; d) P. Ryabchuk, G. Agostini, M.-M. Pohl, H. Lund, A. Agapova, H. Junge, K. Junge, M. Beller, *Sci. Adv.* **2018**, *4*, eaat0761.

[9] a) L. F. B. Ribeiro, O. Flores, P. Furtat, C. Gervais, R. Kempe, R. A. F. Machado, G. Motz, *J. Mater. Chem. A* **2017**, *5*, 720–729; b) C. Bäumler, C. Bauer, R. Kempe, *ChemSusChem* **2020**, *13*, 3110–3114; c) T. Schönauer, S. L. J. Thomä, L. Kaiser, M. Zobel, R. Kempe, *Chem. Eur. J.* **2020**, 1609–1614; d) M. Elfinger, T. Schönauer, S. L. J. Thomä, R. Stäglich, M. Drechsler, M. Zobel, J. Senker, R. Kempe, *ChemSusChem* **2021**, *14*, 2360–2366.

[10] G. Evmenenko, T. T. Fister, D. B. Buchholz, F. C. Castro, Q. Li, J. Wu, V. P. Dravid, P. Fenter, M. J. Bedzyk, *Phys. Chem. Chem. Phys.* **2017**, *19*, 20029–20039.

[11] M. C. Maillard, M. E. Perlman, O. Amitay, D. Baxter, D. Berlove, S. Connaughton, J. B. Fischer, J. Q. Guo, L. Y. Hu, R. N. McBurney, et al., *J. Med. Chem.* **1998**, *41*, 3048–3061.

[12] a) I. Jacquemond-Collet, F. Benoit-Vical, A. Valentin, E. Stanislas, M. Mallié, I. Fourasté, *Planta Med.* **2002**, *68*, 68–69; b) J. H. Rakotoson, N. Fabre, I. Jacquemond-Collet, S. Hannedouche, I. Fourasté, C. Moulis, *Planta Med.* **1998**, *64*, 762–763.

[13] R. J. Pagliero, S. Lusvarghi, A. B. Pierini, R. Brun, M. R. Mazzieri, *Bioorg. Med. Chem.* **2010**, *18*, 142–150.

[14] a) F. Chen, A.-E. Surkus, L. He, M.-M. Pohl, J. Radnik, C. Topf, K. Junge, M. Beller, *J. Am. Chem. Soc.* **2015**, *137*, 11718–11724; b) J. F. S. P. M. V. S. A. Gerster, J. F. S. P. M. U. Gerster, DE2264163 (A1), **1972**; c) J. Bálint, G. Egri, E. Fogassy, Z. Böcskei, K. Simon, A. Gajáry, A. Friesz, *Tetrahedron: Asymmetry* **1999**, *10*, 1079–1087.

Manuscript received: February 5, 2025
Accepted manuscript online: March 12, 2025
Version of record online: April 2, 2025